

Technologies and Materials for Renewable Energy, Environment and Sustainability, TMREES18,
19–21 September 2018, Athens, Greece

A new methodology to model and simulate microgrids operating in low latitude countries

Andrés Julián Aristizábal^{a*}, Jorge Herrera^a, Mónica Castaneda^a, Sebastian Zapata^a, Daniel Ospina^b and Edison Banguero^c

^aDepartment of Engineering, Universidad de Bogotá Jorge Tadeo Lozano, Cr. 4 22-61, Bogotá 110311, Colombia

^bMewbourne College of Earth and Energy, The University of Oklahoma, 660 Parrington Oval, Norman, OK 73019, United States

^cEngineering and Industrial Production Program, Universitat Politècnica de Valencia, Camí de Vera s/n, 46022, Valencia, Spain

Abstract

Energy microgrids have acquired great importance recently thanks to their main characteristics: decentralized generation, use of renewable energy sources in a distributed way, energy storage capacities and the possibility of controlling and managing the use of power flows. This makes the microgrids an excellent option to reduce losses in the transmission and distribution lines and to reduce the use and dependence on fossil fuels worldwide. This article presents a methodology for designing and simulating renewable energy microgrids to operate in countries located near the equator. For this, several mathematical models are proposed for the different components of a microgrid: photovoltaic generator, wind turbine, battery bank and inverter for connection to the electricity grid. Solar and wind resources of five Colombian cities at low latitudes are analyzed: Barranquilla, Santa Marta, Cartagena, Riohacha and Lorica; through NASA's satellite measurement databases. Through the use of neural networks, microgrids are modeled to meet the monthly energy demand of residential users in the proposed cities. The power curves, energy, performance factor and performance variables of the designed systems are presented and discussed. The results allow to validate the excellent energy option represented by microgrids for low-latitude countries, with good rates of solar radiation and wind speed.

© 2019 The Authors. Published by Elsevier Ltd.

This is an open access article under the CC BY-NC-ND license (<https://creativecommons.org/licenses/by-nc-nd/4.0/>)

Selection and peer-review under responsibility of the scientific committee of Technologies and Materials for Renewable Energy, Environment and Sustainability, TMREES18.

* Corresponding author. Tel.: +57-1 242 7030; fax: +57-1 561 2107.

E-mail address: andresj.aristizabal@utadeo.edu.co

Keywords: Microgrids, renewable energy, solar energy, wind energy, battery storage.

1. Introduction

The term smart grid refers to a modernization of the electrical grid consisting in the integration of various technologies such as dispersed generation, dispatchable loads, communication systems and storage devices which operates in grid-connected and islanded modes [1]. Currently, emerging new types of demand-side resources have been spotted in microgrids, including electrical vehicles, air conditioning loads, and refrigerators, which add considerable flexibility to the microgrid operation [2].

Renewable energy sources have been increasingly deployed as distributed generators in remote areas. Meanwhile, fluctuating power generation from renewable energy sources, together with variable power demand, poses challenges in stable and reliable power supply [3]. Microgrids, which are low voltage intelligent distribution grids, have attracted enormous attention from both academia and industry as an effective method to accommodate distributed energy resources (DER) and to reduce the negative effects of renewable energy sources on the entire grid [4].

Access to electricity is a key enabler of social and economic development. However, 1.2 billion people still do not benefit from reliable electricity services. Microgrids have been proposed as a cost-effective means to accelerate access for communities located far from existing grid infrastructure [5]. The successful implementation of microgrids and DER technologies is often subject to various geographic and economic conditions [6].

There are several studies in the literature that address the technical and economic aspects of Microgrids operating in different geographical conditions and operating models [7-14]. This article proposes a methodology to model Microgrids from the meteorological data of the installation city, the user demand and the use of neural networks. In section 2 the microgrid components models are presented. Section 3 describes the operating scenario of the Microgrids and the solar and wind potential for the cities studied; section 4 shows and analyzes the results of the study, and finally in section 5 the conclusions of the investigation are presented.

Nomenclature

DER	Distributed Energy Resources
PV	Photovoltaic
DC	Direct Current
AC	Altern Current
PR	Performance Ratio

2. Modeling microgrid components

2.1 Photovoltaic generator model

The behavior of a solar cell should be evaluated by its performance under darkness and under sunlight illumination. The electric current produced by a solar cell when illuminated is called a photocurrent and is given by the expression:

$$I_{ph} = \frac{G}{1000} [I_{sc} + \Delta i(T - T_r)] \quad (1)$$

Where G represents solar radiation, T and T_r represent the ambient temperature and the reference temperature respectively, Δi represents the temperature coefficient and I_{sc} is the short circuit current defined at a standard temperature.

Because a PV solar module has several solar cells connected to each other, the total current is calculated as:

$$I = I_{ph} - I_s * \left(e^{\left(\frac{V+R_s*I}{n*V_t} \right)} - 1 \right) - \frac{V+R_s*I}{R_{sh}} \quad (2)$$

I_s is the saturation current of a common rectifying diode, V is the saturation voltage, R_s is the series resistor of the module and R_{sh} is shunt resistor module.

The total power of the photovoltaic generator (PPVG) can be calculated by the following expression:

$$P_{PVG} = \frac{E_D}{I_{rrad} * 30 * PR} \quad (3)$$

Where E_D is the monthly energy demanded by the user in kWh/month; I_{rrad} is solar radiation in kWh/m² and PR is the system's performance factor.

2.2 Wind turbine model

Initially the power coefficient must be calculated by the expression [15]:

$$C_p = \frac{2 \cdot P_{wind}}{\lambda \cdot S \cdot V_{wind}^3} \quad (4)$$

The electric power generated by the wind turbine is calculated with equation (5) and the turbine torque by means of equation (6) [16]:

$$P_{wind} = \frac{1}{2} C_p(\lambda) \cdot \rho \cdot S \cdot V_{wind}^3 \quad (5)$$

$$T_{wind} = T_{mec} = \frac{1}{2} \frac{C_p(\lambda) \cdot \rho \cdot R \cdot S \cdot V_{wind}^2}{\lambda} \quad (6)$$

S is the area crossed by the rotor blades (m²), ρ is the air density, R is the radius of the rotor (m), V_{wind} is the wind speed (m/s) and λ is the tip speed ratio.

The permanent magnet synchronous machine model used is given by [17,18]:

$$\begin{bmatrix} V_d \\ V_q \end{bmatrix} = \begin{bmatrix} R_c & -\omega L_c \\ \omega L_c & R_c \end{bmatrix} * \begin{bmatrix} i_d \\ i_q \end{bmatrix} + L_c \frac{d}{dt} \begin{bmatrix} i_d \\ i_q \end{bmatrix} + \begin{bmatrix} e_d \\ e_q \end{bmatrix} \quad (7)$$

The electromagnetic torque can be calculated as:

$$T_{em} = \frac{p}{\omega} (e_q \cdot i_q) = p \cdot \psi_f \cdot i_q \quad (8)$$

where:

e_d, e_q : direct and quadratic magneto driving force, V.

i_d, i_q : direct and quadratic stator currents, A.

V_d, V_q : direct and quadratic stator voltage, V.

L_c : inductance of each stator phase, H.

R_c : resistance of each stator phase, Ω .

2.3 Storage energy device model

The battery bank should have a voltage level that can be calculated as [19,20]:

$$V_{batt} = E_{batt} - R \cdot I_{batt} \quad (9)$$

Where internal battery Voltage E_{batt} is:

During charge: ($i^* < 0$)

$$E_{\text{batt}} = E_0 - k_B \frac{C}{i_t + C} \cdot i^* - k_B \frac{C}{C - i_t} \cdot i_t + \alpha(t) \quad (10)$$

During discharge: ($i^* > 0$)

$$E_{\text{batt}} = E_0 - k_B \frac{C}{C - i_t} \cdot i^* - k_B \frac{C}{C - i_t} \cdot i_t + \alpha(t) \quad (11)$$

$$\alpha(t) = \int \frac{B}{t \cdot (A \cdot I_{\text{batt}} - \alpha(t-1))} \cdot dt \quad (12)$$

This model presumes that during both charge and discharge cycles the voltage is kept constant by the battery's internal resistance [21].

2.4 Grid-connected inverter model

The PV inverter is modelled as a controlled voltage source and it must provide the sinusoidal amplitude values of the output current whereby the power value must be divided by the voltage value provided by the electrical grid at V_{RMS} , because it is being treated as DC power as shown in the following relation:

$$I_{\text{RMS}} = \frac{V_{\text{mpp}} \cdot I_{\text{mpp}} \cdot \eta_f}{V_{\text{redRMS}}} \quad (13)$$

V_{mpp} is the maximum power point at the inverter input and η_f is the efficiency of the inverter.

2.5 Electrical grid model

This proposed model is an RLC circuit whose main characteristic must be having a power factor greater than or equal to 0.85 as established by the IEEE 929-2000 standard. To meet such a requirement, an impedance value is first set to the appropriate angle with equation (14).

$$\theta = \arccos(0.85) = 31.7^\circ \approx 30^\circ \quad (14)$$

Taking expression (15) into account, values are established for $R = 3\Omega$ and $X = \sqrt{3}$. The values of the inductive (X_L) and capacitive (X_C) reactance are calculated considering the expressions (16) and (17) at a frequency of 60Hz.

$$\tan\theta = \frac{(X_L - X_C)}{R} = \frac{\sqrt{3}}{3} \quad (15)$$

$$X_C = \frac{1}{2 \cdot \pi \cdot f \cdot C} \quad (16)$$

$$X_L = 2\pi f L \quad (17)$$

An inductance value of $L = 2\text{H}$ is established for the purpose of having a positive reactive power and the expression (18) is used to obtain the value of the capacitance (C) where $w = 2\pi f L$.

$$C = \frac{1}{\omega^2 L - \omega \sqrt{3}} = 3.526 \cdot 10^{-6} \text{F} \quad (18)$$

3. Microgrids analysis scenario

3.1 Solar and wind potential

The first step in the proposed methodology is to define the meteorological conditions of the cities in which the renewable energy microgrids will be installed. The cities selected to apply the proposed methodology are cities located on the Atlantic coast of Colombia and have excellent conditions of solar radiation and wind speed because they border the Caribbean Sea. Table 1 shows the geographical location of the selected cities.

Table 1. Geographical coordinates of the study cities. Source: Authors

City	Latitude	Longitude
Barranquilla	10.980220	-74.829420
Cartagena	10.420627	-75.552159
Santa Marta	11.232997	-74.220535
Riohacha	11.541336	-72.931994
Lorica	9.245795	-75.821950

Figures 1, 2 and 3 show the monthly profiles of solar radiation, ambient temperature and wind speed for the selected cities. The data were obtained directly from the NASA databases [22] "Prediction of Worldwide Energy Resources" and correspond to meteorological data measured during the last 22 years.

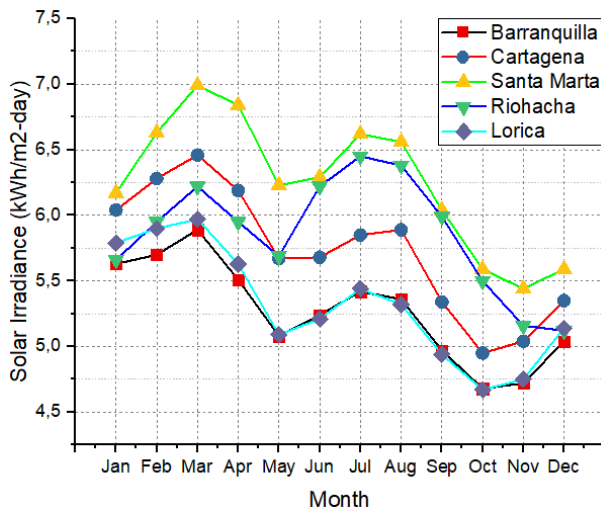


Fig. 1. Monthly solar radiation profile for selected cities. Source: Authors.

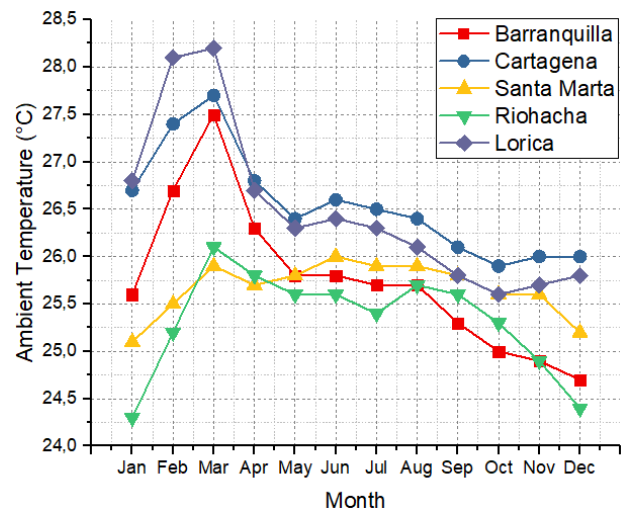


Fig. 2. Monthly ambient temperature profile for the selected cities. Source: Authors.

The city of Santa Marta presents the greatest potential of solar radiation with an annual average of 6.25 kWh/m²-day; while the cities of Barranquilla and Lorica have the lowest with a value of 5.27 kWh/m²-day and 5.32 kWh/m²-day respectively.

The ambient temperature must be taken into account in the design of photovoltaic systems because it affects the open circuit voltage of the solar cells. In all the cities of the study, the ambient temperature varies between 24.3 °C and 28.2 °C.

The wind speed reported in Fig. 3 that allows to evaluate the wind potential of the 5 cities, was measured at a height of 50m. Santa Marta also has the highest wind potential in the cities analyzed with an annual average of 15.6 m/s and in second place the city of Riohacha with an annual average of 15.3 m/s. Lorica has the lowest wind potential with 13.6 m/s.

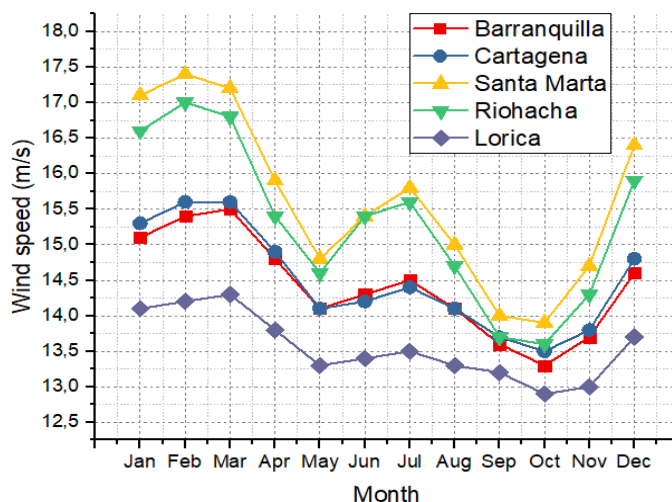


Fig. 3. Monthly wind speed profile for the selected cities. Source: Authors.

3.2 Energy demand

Once the potential of renewable energy in each city was assessed, the monthly energy demand for a certain number of residential users was defined, to be covered by the Microgrids. Residential users of type 4 stratum in Colombia were selected, because they represent one of the largest consumers of residential energy in the country. Table 2 shows the monthly energy consumption for residential users, stratum 4, for the cities analyzed.

Table 2. Monthly energy demand for 1 residential user from stratum 4, in the 5 cities, 2017. Source: SUI – UPME [23].

Month, 2017	Monthly energy demand (kWh/month) Barranquilla	Monthly energy demand (kWh/month) Cartagena	Monthly energy demand (kWh/month) Santa Marta	Monthly energy demand (kWh/month) Riohacha	Monthly energy demand (kWh/month) Loricá
January	346.17	371.61	386.78	444.66	392.54
February	299.86	328.74	327.66	286.04	374.50
March	315.82	367.53	354.38	288.25	456.51
April	359.50	416.66	427.74	371.58	526.95
May	383.85	392.61	398.39	353.69	430.43
June	398.15	401.34	397.11	358.29	423.21
July	402.88	420.43	409.24	403.33	424.39
August	395.39	407.03	398.98	370.62	402.97
September	417.75	398.39	383.70	408.22	412.95
October	401.29	402.12	377.25	388.68	388.60
November	404.11	403.90	388.99	439.89	398.66
December	377.47	348.56	353.01	349.36	375.99
Maximum demand	417.75	420.43	427.74	444.66	526.95
Demand 15 users (households)	6266.25	6306.45	6416.10	6669.90	7904.25

The high values of monthly energy demand in Table 2 are partly due to the high temperatures of the cities evaluated (see Fig. 2) where users must use air conditioning systems in their homes during the day. Because 1 user corresponds to 1 house (household), in this study it is proposed for each city, to create residential sets of 15 houses, for which the Microgrids will be dimensioned in order to meet their monthly energy needs: 70% of the monthly demand will be supplied by photovoltaic solar energy and the remaining 30% of the monthly demand will be produced through wind energy. In case the wind energy produced is not enough to cover the demand, the microgrid will use the energy stored in the batteries and in the extreme case that the batteries do not have energy at that moment, the necessary surplus of energy will be consumed from the electrical grid. It is assumed that the Microgrids will be installed in an appropriate space for their operation near the residential complexes, where the wind turbines and other equipment do not represent a danger to people and houses. Table 2 shows the maximum monthly energy for each house in the 5 cities as well as the monthly demand for 15 houses. For example: for Barranquilla the maximum

monthly demand of a house is 417.25 kWh/month and therefore, the monthly demand for 15 houses will be 6266.25 kWh/month, 70% of this demand will be supplied with PV energy, (4386.38 kWh/month) and the remaining 30% (1879.88 kWh / month) with wind energy.

3.3 Modeling microgrids using neural networks

Fig. 4 shows the design of the microgrid for each city, modeled by neural networks.

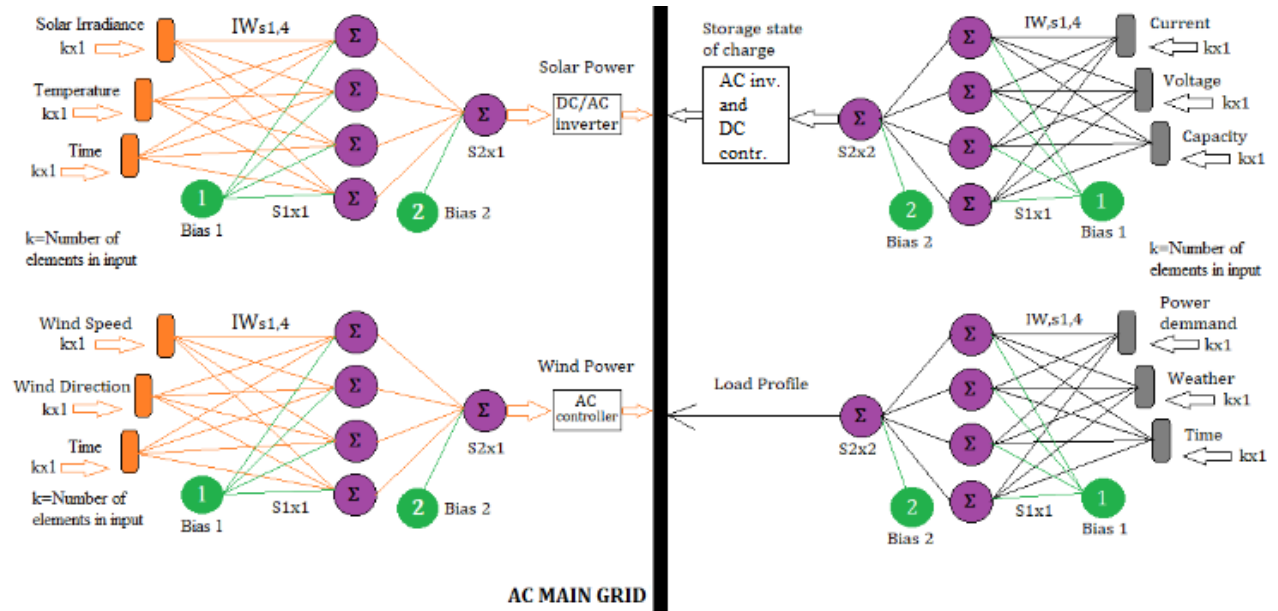


Fig. 4. Structure of neural networks for microgrids simulation. Source: Authors.

The complete system of the microgrid is divided into four subsystems: solar energy, wind energy, batteries and user load. Each system has been modeled by the use of neural networks. For the solar energy subsystem, the input variables are: solar radiation, ambient temperature and time series. For the wind energy subsystem the input variables are: wind speed, wind direction and time series. The input variables of the battery subsystem are: the electric current, the voltage and the capacity of the batteries (each one with its respective time). The input variables for the user's load are: the power demand, the climatic variations and the time series. The use of the minimum neural network that can learn the task, in the end provides better results for both theoretical and practical reasons. Each system was trained using a neuronal network of 4 input neurons, 12 hidden neurons and one output. After an analysis that allowed to evaluate the error during the training of the neural networks, it was concluded that the best window size for each signal was 4. The activation algorithm for the neural networks was the Log-Sigmoid function, while each output was worked with a linear function. The training stage of the user's load subsystem was carried out under different operating scenarios, because of the hot climate of the studied cities, the power consumption is high due to refrigeration equipment and the other home appliances do not have a normalized schedule for their use.

Additionally, it was necessary to establish patterns of switching on and off of electrical appliances. Obtain each output of each subsystem, required to configure the input layer as a vector in the three-dimensional space that includes as columns the three input variables and where k represents the index of the sample data.

3.4 Microgrids description

In order to model the micro networks, solar panels and inverter AC / DC Tanfon Energy™ brand were used thanks to its reliability, price and availability in the Market. Table 3 shows the electrical specifications of the solar panels used.

Table 3. Technical specifications of the used solar panels.

Electrical Data - STC	
PV MODULE	FS330P-24
Nominal Maximum Power (Pmax) [W]	330
Optimum Operating Voltage (Vmp) [V]	37.4
Optimum Operating Current (Imp) [A]	8.83
Open Circuit Voltage (Voc) [V]	45.2
Short Circuit Current (I _{sc}) [A]	9.86
Module Efficiency (η) [%]	15.5

Table 4 presents the electrical characteristics of the inverter chosen for the study.

Table 4. Technical specifications of the inverter used.

Electrical Data - STC	
AC/DC Inverter	HBF10K
Nominal Power [W]	10000
Max. DC Power [kW]	10.4
Rated AC Voltage [V]	220V
Rated Frequency [Hz]	60
THD [%]	< 2
Efficiency (η) [%]	97.4

Table 5 presents the specifications of the other components of the microgrids.

Table 5. Specifications of each subsystem of the micro grid.

Wind generator	Values
Power rating	10 000 Wp
Radius of the turbine	7 m
Battery bank	
Capacity	28 000 Wp @ 12 h
Rated voltage	48 V
Load	
Minimum demand	100 kWh/month
Maximum demand	10 000 kWh/month

These equipment specifications were used in the mathematical models of the equations for each component of the microgrids presented in chapter 2 in order to dimension the subsystems. The proposed algorithm is responsible for dimensioning the subsystems: the total power of each photovoltaic and wind generator, the capacity of the batteries and the inverters. The values specified in Tables 3 to 5 are the minimum values. Regarding the electrical grid, technical specifications stipulated in the Colombian Electric Code NTC 2050 were used.

These results are integrated with the meteorological signals and with the neural network model to obtain the results of the simulation of the performance of microgrids in the cities analyzed.

4. Simulation results

Fig. 5 shows the DC energy generation from the microgrids' photovoltaic generators for each of the cities analyzed.

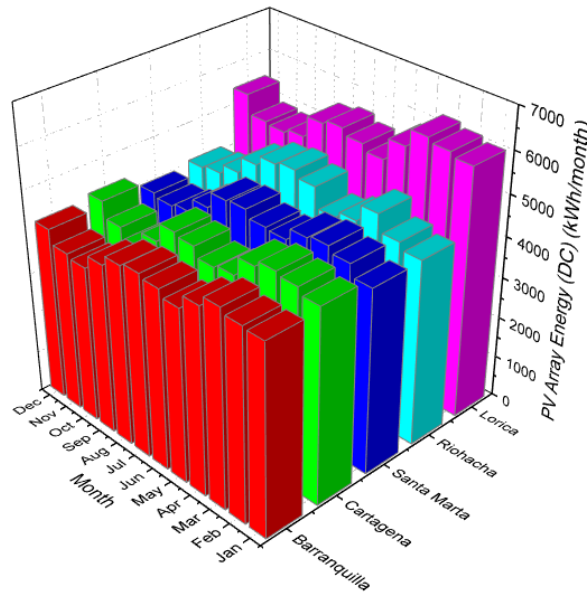


Fig. 5. Monthly profile of DC photovoltaic generation in the cities studied. Source: Authors.

As proposed in the model, 70% of the load's monthly demand is supplied using the photovoltaic generators. Due to the fact that the city of Loricá has the highest monthly energy demand (7904.25 kWh/month), the PV generator of its microgrid produces a range of energy throughout the year ranging from 4905.39 kWh/month to 6262.2 kWh/month. Barranquilla, which is the city with the lowest energy demand (6266.25 kWh/month), has an average DC power generation of 4347.29 kWh/month. In the other cities, the generation of pv energy is intermediate and its production is guaranteed thanks to the excellent solar potential recorded.

Figure 6 shows the AC pv energy of the microgrids, that is, the energy at the inverter output of each photovoltaic array.

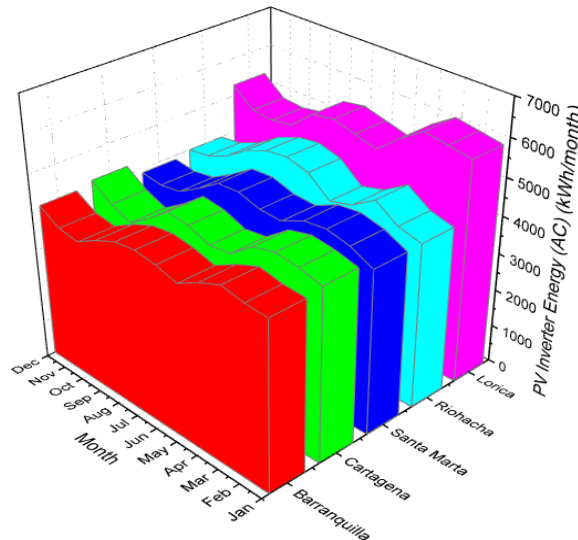


Fig. 6. Monthly profile of the AC photovoltaic generation in the cities studied. Source: Authors

As expected, the energy produced at the output of the inverters is lower due to the losses recorded by the DC/AC electrical conversion. The model uses the conversion efficiency of the inverters that is presented in Table 4, which is 97.4%. This energy is managed by the management and control system of each monitoring that, according to the load consumption scenarios, manages the direct use towards the users or towards the battery bank through isolated autonomous inverters.

Fig. 7 shows the performance ratio (PR) for each of the photovoltaic generators.

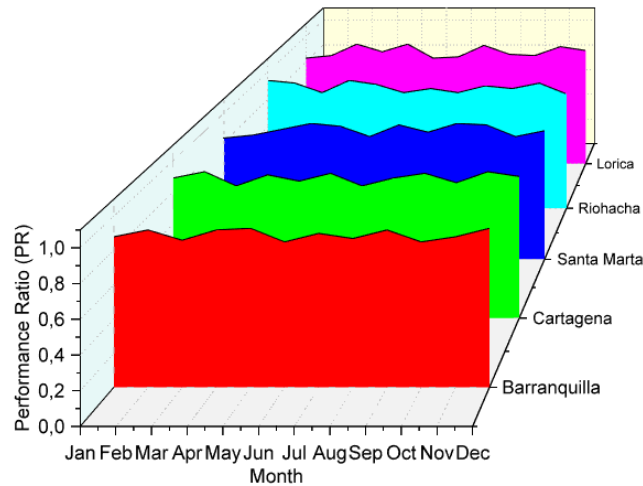


Fig. 7. Performance ratio (PR) of the photovoltaic generators. Source: Authors

The performance ratio is a measure of the quality of the photovoltaic plant, which evaluates the relationship between real energy and theoretical energy production. In all the cities evaluated, the PR factor exceeded the value of 0.83 with a maximum value of 0.94 in the cities of Riohacha and Lorica. These values already have all the Losses by generation of energy in the solar panels, the DC/AC conversion and the wiring.

Fig. 8 shows the wind energy generated monthly in each of the microgrids studied.

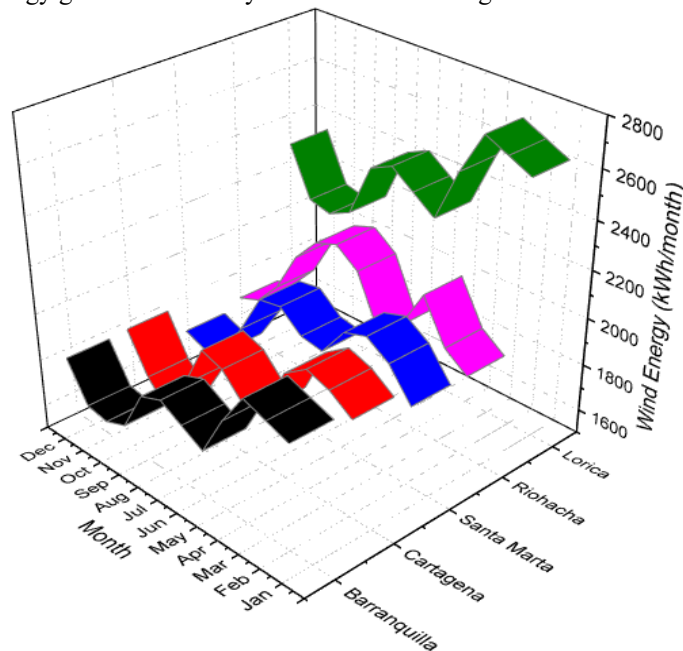


Fig. 8. Wind power generated per month in each microgrid. Source: Authors

Wind generation in each microgrid must supply 30% of the demand as proposed in the model. In the microgrid of the city of Lorica, the minimum wind energy generated is presented in the month of October with a value of 2115 kWh/month, while the maximum value is reached in the month of March with 2700 kWh/month. In second place is the city of Riohacha, which registers a yearly average of 2006.75 kWh/month. In the city of Santa Marta, wind production ranges between 1684.8 kWh/month and 2121.6 kWh/month. Cartagena and Barranquilla have very similar values of wind generation, ranging on average as 1886.5 kWh/month and 1882.1 kWh/month respectively.

Fig. 9 shows the effective current (Irms) in each of the microgrids; while Fig. 10 shows the energy stored in the battery banks for each city.

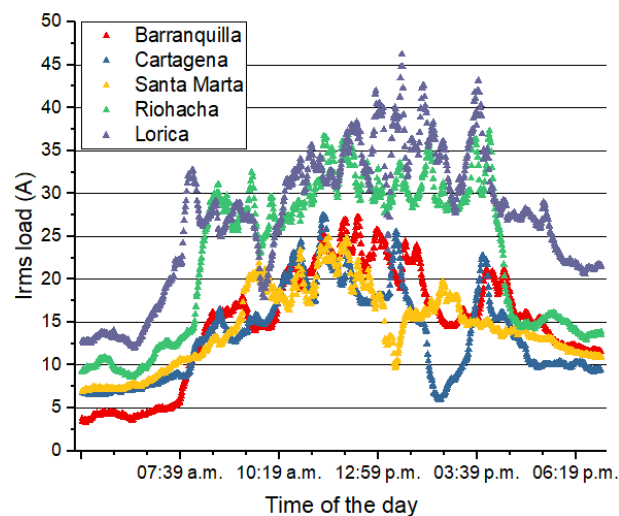


Fig. 9. Daily profile of effective current consumed by the load for the cities studied. Source: Authors.

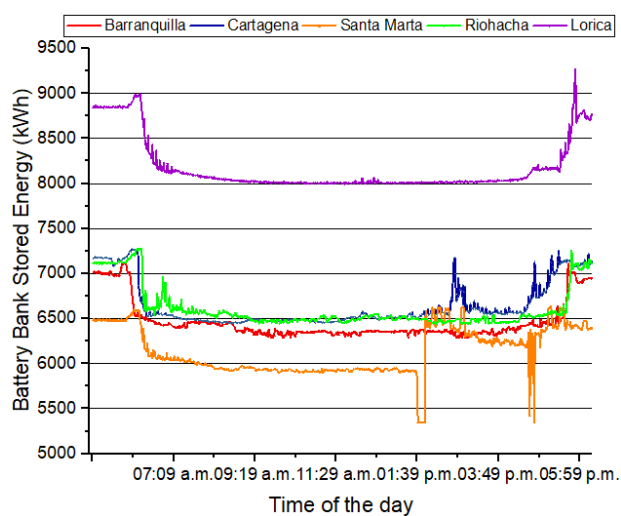


Fig. 10. Daily profile of energy stored in batteries for the cities studied. Source: Authors.

The behavior of the load current of the user is due to the different on / off scenarios that were simulated, in order that these coincided with the greater availability of photovoltaic solar resource in the 5 cities of the study. The management and control system of the microgrids is responsible for optimizing the use of energy resources so that during the daytime hours photovoltaic generation goes directly to the load and in the case of surplus energy, it is stored directly in the batteries. However, also within the current consumed by the load is already included 30% of the contribution made by wind generation.

As for the battery bank, the programmed operating scenarios guarantee that the minimum energy demand required by each user is available in storage for a day of autonomous operation, as can be seen in Fig. 10. Battery autonomy was not increased in order to avoid additional expenses. It is observed that at 6 am, the user's load begins to consume energy from the batteries (this was defined as one hour of maximum consumption of the batteries) and at the end of the afternoon and during the night, its storage is increased by the wind generation, taking into account that there is a percentage of losses associated with the ac / dc conversion of the wind generators.

Acknowledgements

This work was supported by Universidad de Bogotá Jorge Tadeo Lozano under grant 830-15-17.

Conclusions

The model of the different components that integrate the microgrids offers the simplicity to size systems of any power and allows the user to select according to their economic or technical convenience, solar panels, wind turbine, batteries and inverters.

Through the use of neural networks it was possible to design microgrids for five Colombian cities with different potentials of solar radiation and wind speed. The proposed grid allows obtaining profiles of generated energy, battery bank behavior and the user's load.

The methodology proposed for low-latitude cities involves the selection of those that have appropriate sun and wind resources. In Colombia there are good levels of solar radiation in most cities, but the best wind conditions only occur in the regions of the Atlantic coast. The model can be applied to cities in the interior of the country, but a substitute for wind energy should be evaluated, which could be through the use of biomass or using fossil fuels such as diesel generation, which should be evaluated according to the objectives of the research. .

The study presented in this article can be used as a preliminary analysis for the installation of hybrid generation systems in Colombia, since through Law 1715 of 2014, any Colombian citizen can install clean energy generation systems, accessing tax incentives for the purchase of the equipment and additionally can sell to the electricity company the surplus energy generated by their systems.

References

- [1] H. Abdi, S. D. Beigvand, and M. La Scala, "A review of optimal power flow studies applied to smart grids and microgrids," *Renew. Sustain. Energy Rev.*, vol. 71, no. May 2015, pp. 742–766, 2017.
- [2] Y. Du, F. Li, X. Kou, and W. Pei, "Coordinating multi-microgrid operation within distribution system: A cooperative game approach," *IEEE Power Energy Soc. Gen. Meet.*, vol. 2018–January, no. December 2017, pp. 1–5, 2018.
- [3] J. Hu, Y. Xu, K. Wai, and J. M. Guerrero, "A model predictive control strategy of PV-Battery microgrid under variable power generations and load conditions," *Appl. Energy*, vol. 221, no. February, pp. 195–203, 2018.
- [4] Y. Zhang, F. Meng, R. Wang, W. Zhu, and X.-J. Zeng, "A Stochastic MPC based Approach to Integrated Energy Management in Microgrids," *Sustain. Cities Soc.*, vol. 41, no. May, pp. 349–362, 2018.
- [5] N. J. Williams, P. Jaramillo, and J. Taneja, "An investment risk assessment of microgrid utilities for rural electrification using the stochastic techno-economic microgrid model: A case study in Rwanda," *Energy Sustain. Dev.*, vol. 42, pp. 87–96, 2018.
- [6] Q. Kong, M. Fowler, E. Entchev, and H. Ribberink, "Impact assessment of microgrid implementation considering complementary building operation: An Ontario, Canada case," *Energy Convers. Manag.*, vol. 168, no. May, pp. 564–575, 2018.
- [7] F. Guzzi, D. Neves, and C. A. Silva, "Integration of smart grid mechanisms on microgrids energy modelling," *Energy*, vol. 129, pp. 321–330, 2017.
- [8] E. Bullich-Massagué, F. Díaz-González, M. Aragüés-Peñalba, F. Girbau-Llistuella, P. Olivella-Rosell, and A. Sumper, "Microgrid clustering architectures," *Appl. Energy*, vol. 212, no. November 2017, pp. 340–361, 2018.
- [9] A. Alzahrani, M. Ferdowsi, P. Shamsi, and C. H. Dagli, "Modeling and Simulation of Microgrid," *Procedia Comput. Sci.*, vol. 114, pp. 392–400, 2017.
- [10] V. Bhattacharjee and I. Khan, "A non-linear convex cost model for economic dispatch in microgrids," *Appl. Energy*, vol. 222, no. January, pp. 637–648, 2018.
- [11] Z. Zeng, R. Zhao, H. Yang, and S. Tang, "Policies and demonstrations of micro-grids in China: A review," *Renew. Sustain. Energy Rev.*, vol. 29, pp. 701–718, 2014.
- [12] A. J. Aristizábal, C. A. Páez, and D. H. Ospina, *Building Integrated Photovoltaic Systems*. Springer International Publishing AG, 2018.
- [13] Aristizábal, A.J. and Páez, C.A., 2017. Experimental investigation of the performance of 6 kW BIPV system applied in laboratory building. *Energy and Buildings*, 152, 1-10.
- [14] Aristizábal, J. and Gordillo, G. Performance and economic evaluation of the first grid - connected installation in Colombia over 4 years of continuous operation. *International Journal of Sustainable Energy*, 30 (1), 34-46.
- [15] A. Tomilson, J. Quaicoe, R. Gosine, M. Hinchey and N. Bose, "Modelling an autonomous wind-diesel system using simulink". In: *Electrical and computer engineering. Engineering innovation: voyage of discovery. IEEE 1997 Canadian conference*, pp. 35-38, 1997.
- [16] B. Belvedere, M. Bianchi, A. Borghetti, C.A. Nucci, M. Paolone and A. Peretto, "A microcontroller-based power management system for standalone micro grids with hybrid power supply". *IEEE Trans Sustain Energy*, vol. 3 (3), 422-431, 2012.
- [17] A. Mohammedi, N. Mezzai, D. Rekioua and T. Rekioua, "Impact of shadow on the performances of a domestic photovoltaic pumping system incorporating an MPPT control: a case study in Bejaia, North Algeria". *Energy Convers Manag*, vol. 84, pp. 20-29, 2014.
- [18] D. Rekioua and E. Matagne, "Optimization of photovoltaic power systems: modelization, simulation and control". *Green Energy Technol*, 102, 2012.
- [19] M. Bechouat, Y. Soufi, M. Sedraoui and S. Kahla, "Energy storage based on maximum power point tracking in photovoltaic systems: A comparison between GAs and PSO approaches". *Int J Hydrog Energy*, 2015.
- [20] H. Fathabadi, "Fuel cell/back-up battery hybrid energy conversion systems: dynamic modeling and harmonic considerations". *Energy Convers Manag*, vol. 103, pp. 573-584, 2015.
- [21] A. Rezvani, A. Khalili, A. Mazareie and M. Gandomkar, "Modeling, control and simulation of grid connected intelligent hybrid battery/photovoltaic system using new hybrid fuzzy-neural method". *ISA Transactions*, vol. 63, pp. 448-460, 2016.
- [22] NASA Prediction of Worldwide Energy Resources, Power project data sets, NASA, July 2018. Available: <https://power.larc.nasa.gov> (Accessed: 12/02/2017).
- [23] Sistema Único de Información de Servicios Públicos Domiciliarios - SUI,. Available online at www.sui.gov.co. Accessed on 24/07/2018.